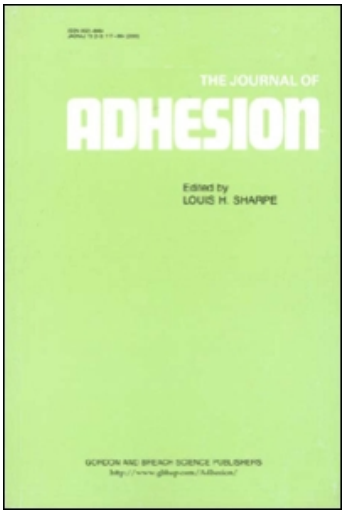

The Journal of Adhesion
Publication details, including instructions for authors and subscription information:
http://www.informaworld.com/smpp/title~content=t713453635

Peeling Pressure-Sensitive Adhesive Tape from Thin Elastic Strip

Raymond H. Plaut[a]
[a] Department of Civil and Environmental Engineering, Virginia Polytechnic Institute and State University, Blacksburg, Virginia, USA

Online publication date: 10 August 2010

To cite this Article Plaut, Raymond H.(2010) 'Peeling Pressure-Sensitive Adhesive Tape from Thin Elastic Strip', The Journal of Adhesion, 86: 7, 675 — 697
To link to this Article: DOI: 10.1080/00218464.2010.482387
URL: http://dx.doi.org/10.1080/00218464.2010.482387

The Journal of Adhesion, 86:675–697, 2010

ISSN: 0021-8464 print/1545-5823 online
DOI: 10.1080/00218464.2010.482387

Taylor & Francis
Taylor & Francis Group

Peeling Pressure-Sensitive Adhesive Tape from Thin Elastic Strip

Raymond H. Plaut
Department of Civil and Environmental Engineering,
Virginia Polytechnic Institute and State University,
Blacksburg, Virginia, USA

In some applications of peeling of a pressure-sensitive adhesive tape, the substrate is thin and flexible, such as fabric, paper, leather, rubber, or skin. A thin strip, fixed at its ends, is considered as the substrate in this study. The strip and tape are assumed to be linearly elastic with negligible bending stiffness. The peel force depends on the adhesive fracture energy, the axial stiffnesses of the tape and strip, the initial slack of the strip, the initial location and length of the tape attached to the strip, and the peel angle of the force with respect to the line connecting the supports (or the local peel angle with respect to the side of the strip to which the tape is attached). Additional analyses involving an inextensible tape or an inextensible strip are included, along with an experimental result. The effects of various nondimensional parameters on the peel force are investigated.

Keywords: Fracture mechanics; Peel force; Pressure-sensitive adhesive; PSA; Thin flexible substrate

1. INTRODUCTION

Most analyses of peel tests involve peeling a pressure-sensitive adhesive tape from a rigid substrate [1]. In some applications, however, the substrate is thin and flexible. The motivation for the present study is the peeling of medical adhesives from skin [2,3], and peeling of tape from a sheet of fabric, paper, leather, or rubber.

Received 22 August 2009; in final form 10 December 2009.

One of a Collection of papers honoring David A. Dillard, the recipient in February 2010 of *The Adhesion Society Award for Excellence in Adhesion Science, Sponsored by 3M*.

Address correspondence to Raymond H. Plaut, Department of Civil and Environmental Engineering, Virginia Polytechnic Institute and State University, MC 0105, Blacksburg, VA 24061, USA. E-mail: rplaut@vt.edu

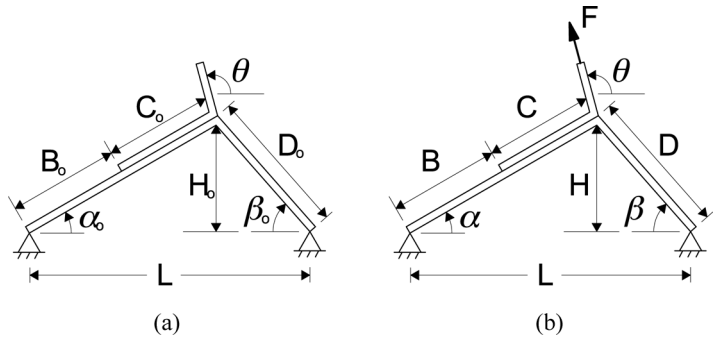

FIGURE 1 Illustration of system (a) before loading and (b) under load.

The two-dimensional system is sketched in Fig. 1. The initial configuration is shown in Fig. 1(a), where the span is L, the initial length of the strip is $B_o + C_o + D_o$, and the initial angles of the strip segments with the horizontal are α_o and β_o. The bending stiffness and self-weight of the strip and of the tape are neglected, so the segments are straight. The attached length of the tape is initially C_o. The deformed configuration is depicted in Fig. 1(b), where a force, F, is applied to the end of the detached portion of the tape at a peel angle, θ, with the horizontal (*i.e.*, not with the substrate). The strip and tape are assumed to be linearly elastic, and the effect of the peel rate is not considered in the analysis.

In Roop *et al.* [4], a similar system was analyzed for the case $B_o = 0$ and an inextensible strip that was initially slack. Some experimental results were reported, and another set of those results will be presented here. In Steven-Fountain *et al.* [5], the system in Fig. 1 was analyzed for the case of an inextensible tape, peel angle $\theta = 0.5\pi$, and no initial slack (*i.e.*, $B_o + C_o + D_o = L$). Both linearly and nonlinearly elastic models were included for the strip, and some experimental results were described. The criterion for peeling in the analyses of [4] and [5] was based on fracture mechanics, and the same criterion will be used here.

Attention will be focused on the effects of the following parameters on the nondimensional peel force: peel angle, θ; nondimensional length, B_o/L, of the strip without tape on the left side in Fig. 1(a); slackness parameter, $s_o = (B_o + C_o + D_o)/L$; nondimensional adhesive fracture energy; and relative axial stiffness between the tape and the strip. Some results for the increase in peel force prior to peeling will also be presented.

The analysis will be formulated in Section 2. In Section 3, numerical results will be presented for the general case in which both the strip and tape are extensible. The case of an inextensible tape will be

treated in Section 4, and an inextensible strip will be considered in Section 5. Experimental results will be described in Section 6, followed by concluding remarks in Section 7.

2. FORMULATION

For the unloaded system shown in Fig. 1(a), the initial height of the strip is H_o, the initial length of the strip is denoted S_o, and the other parameters have been defined in the previous section. For the loaded system in Fig. 1(b), the stretched length of the strip on the left side with no tape is B, the stretched length of the strip with attached tape is C, the stretched length of the strip on the right side is D, the height of the strip is H, and the left and right angles of the strip with the horizontal are α and β, respectively. When peeling occurs, the peel force is denoted F_p.

The moduli of elasticity for the strip and tape are E_s and E_t, respectively, and the corresponding cross-sectional areas are A_s and A_t. The length of the tape will not be involved in the results for cases in which both the strip and tape are extensible; it will be assumed for those cases that the initial tape length is the same as the initial strip length, so that the axial stiffnesses are E_tA_t/S_o for the tape and E_sA_s/S_o for the strip, and the ratio E_tA_t/E_sA_s will be called the "stiffness ratio" and denoted η.

The width of the strip and also of the tape is w. The values of the axial forces in the segment of the strip with length B, the segment of the tape and strip with length C, the strip segment with length D, and the detached tape, respectively, are denoted N_b, N_c, N_d, and N_r. The adhesive fracture energy (*i.e.*, the critical value of the strain energy release rate) is G_c.

The analysis is conducted in terms of the nondimensional quantities

$$b_o = \frac{B_o}{L}, \quad c_o = \frac{C_o}{L}, \quad d_o = \frac{D_o}{L}, \quad h_o = \frac{H_o}{L}, \quad s_o = \frac{S_o}{L}, \quad b = \frac{B}{L}, \quad c = \frac{C}{L}, \quad d = \frac{D}{L},$$
$$h = \frac{H}{L}, \quad n_b = \frac{N_b}{E_sA_s}, \quad n_c = \frac{N_c}{E_sA_s}, \quad n_d = \frac{N_d}{E_sA_s}, \quad n_r = \frac{N_r}{E_sA_s}, \quad f = \frac{F}{E_sA_s},$$
$$f_p = \frac{F_p}{E_sA_s}, \quad f^* = \frac{F}{E_tA_t}, \quad f_p^* = \frac{F_p}{E_tA_t}, \quad g_c = \frac{G_cw}{E_sA_s}, \quad g_c^* = \frac{G_cw}{E_tA_t}, \quad \eta = \frac{E_tA_t}{E_sA_s},$$
$$\phi = \theta - \alpha, \tag{1}$$

where ϕ is the "local peel angle" between the applied force and the left side of the strip. The initial and equilibrium lengths of the strip are

$$B_o + C_o + D_o = S_o, \quad b_o + c_o + d_o = s_o, \tag{2}$$

respectively, with the slackness parameter $s_o \geq 1$.

The engineering strains for the segments with lengths B, C, and D, and the detached tape segment are

$$\varepsilon_b = \frac{b - b_o}{b_o}, \quad \varepsilon_c = \frac{c - c_o}{c_o}, \quad \varepsilon_d = \frac{d - d_o}{d_o}, \quad \varepsilon_r = \frac{f}{\eta}, \tag{3}$$

respectively, and the corresponding nondimensional axial forces are

$$n_b = \varepsilon_b, \quad n_c = (1 + \eta)\varepsilon_c, \quad n_d = \varepsilon_d, \quad n_r = f, \tag{4}$$

all of which must be positive (corresponding to tension) for the model to be applicable.

Based on the geometry of Fig. 1(b),

$$(b + c)\cos\alpha + d\cos\beta = 1, \tag{5}$$

$$(b + c)\sin\alpha = d\sin\beta. \tag{6}$$

Equations (5) and (6) can also be used for the initial configuration to obtain the angles α_o and β_o for given values of the lengths b_o, c_o, and d_o.

Based on equilibrium at the transition between the segments of length B and C in Fig. 1(b),

$$n_b = n_c. \tag{7}$$

At the top of the strip, equilibrium of components perpendicular to the force yields

$$n_c \sin(\theta - \alpha) = n_d \sin(\theta + \beta), \tag{8}$$

and vertical equilibrium furnishes

$$f \sin\theta = n_c \sin\alpha + n_d \sin\beta. \tag{9}$$

Prior to peeling, for given values of the peel angle, θ, the nondimensional initial lengths b_o, c_o, and d_o (and, hence, the slackness parameter, s_o), and the stiffness ratio, η, the relationship between the applied force, f, and the angle, α (or another parameter), can be computed using Eqs. (5)–(9), with the use of Eqs. (3) and (4) to write the axial forces n_b, n_c, and n_d in terms of lengths. Numerical solutions are obtained using *Mathematica* [6].

When peeling occurs, consider detachment of an incremental length Δa of the tape from the left side of the peak of the strip. The subsequent lengths and angles are denoted with a prime, and are written as

$$b' = b + \Delta b, \quad c' = c - \Delta a, \quad d' = d + \Delta d, \quad \alpha' = \alpha + \Delta\alpha, \quad \beta' = \beta + \Delta\beta. \tag{10}$$

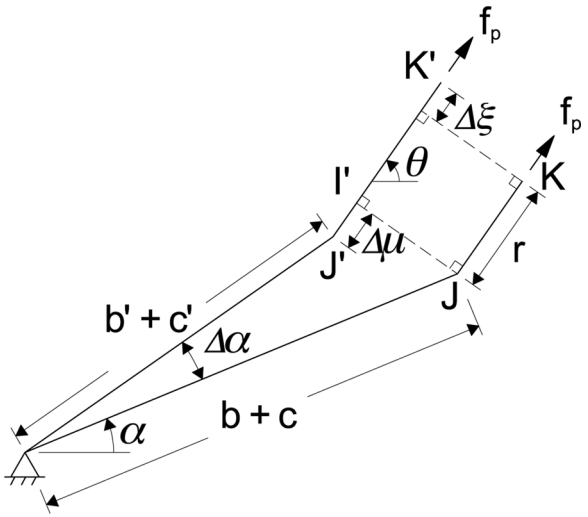

FIGURE 2 Left side of strip before and after incremental peeling.

A linear analysis is used with Eqs. (5)–(8) to obtain the incremental changes in b, d, α, and β in terms of Δa, and the resulting relationships have the general form

$$\Delta b = k_b \Delta a, \quad \Delta d = k_d \Delta a, \quad \Delta \alpha = k_\alpha \Delta a, \quad \Delta \beta = k_\beta \Delta a. \tag{11}$$

The coefficients k_b, k_d, k_α, and k_β are lengthy and are not listed here.

In nondimensional terms, Fig. 2 depicts the left side of the strip before and after the incremental change of the configuration. The length of the detached tape before the incremental change is denoted r. After the change, the length is $r + \Delta\mu + \Delta\xi$. The angle of the detached tape with the horizontal is θ. Making use of the equations of the line segments I′J and I′J′, it can be shown that the length $\Delta\mu$ in terms of Δa is

$$\Delta\mu = [\cos(\theta - \alpha) - k_\alpha c \sin(\theta - \alpha)]\Delta a. \tag{12}$$

The dimensional energies are divided by $E_s A_s L$ to give the nondimensional energies. The nondimensional strain energies for the segments with dimensional lengths B, C, and D are denoted U_b, U_c, and U_d, respectively, and are given by

$$U_b = \frac{(b' - b_o)^2 b'}{2b_o^2}, \quad U_c = \frac{(c' - c_o)^2 c'}{2c_o^2}, \quad U_d = \frac{(d' - d_o)^2 d'}{2d_o^2}. \tag{13}$$

The incremental change in the nondimensional strain energy associated with stretching of the detached tape is

$$\Delta U_r = \frac{f^2 \Delta a}{2\eta}. \tag{14}$$

The nondimensional incremental work done by the force is

$$\Delta W = f\Delta a + \frac{f^2}{\eta}\Delta a - f\Delta\mu, \tag{15}$$

and the nondimensional required fracture energy is

$$\Delta\Gamma = g_c \Delta a. \tag{16}$$

For steady peeling [7],

$$\Delta\Gamma + \Delta U_b + \Delta U_c + \Delta U_d + \Delta U_r - \Delta W = 0. \tag{17}$$

In Eq. (17), the incremental formulas in U_b, U_c, and U_d are linearized in the incremental lengths, all expressions are written in terms of Δa, and the resulting equation is divided by Δa.

The nondimensional peel force $f = f_p$ can be obtained numerically. Values of peel angle θ, initial lengths b_o, c_o, and d_o, stiffness ratio η, and nondimensional adhesive fracture energy g_c are specified. With the use of Eqs. (3) and (4), Eqs. (5)–(9) and (17) can be solved for α, β, b, c, d, and f_p.

3. RESULTS FOR GENERAL CASE

3.1. Effect of Initial Attached Length of Tape

On the left side of the strip, in nondimensional terms, the initial length of the strip to the left of its peak is $b_o + c_o$, with the tape not attached for the length b_o [see Fig. 1(a)]. The effect of b_o on the nondimensional peel force, f_p, is investigated in this subsection.

In Figure 3, $\theta = 0.75\pi$, $s_o = 1$ (no initial slack), $d_o = 0.5$ (half the original strip length), $g_c = 0.01$, and $\eta = 0.5$, 2, and 10. Therefore, the length of the strip to the left of the tape, b_o, can vary from 0 (when the tape is attached to half of the strip) to 0.5, and the attached length is $c_o = 0.5 - b_o$. For this situation, the peel force is higher when the attached length is longer (*i.e.*, when b_o is smaller). When $b_o = 0$, $f_p = 0.0126$, 0.0153, and 0.00958, respectively, for $\eta = 0.5$, 2, and 10.

Similar results are presented in Fig. 4 for the case $\theta = 0.5\pi$ (vertical force), $s_o = 1.4$, $d_o = 0.7$ (half the original strip length), $g_c = 0.01$, and $\eta = 0.5$, 2, and 10. Therefore, b_o can vary from 0 to 0.7, and

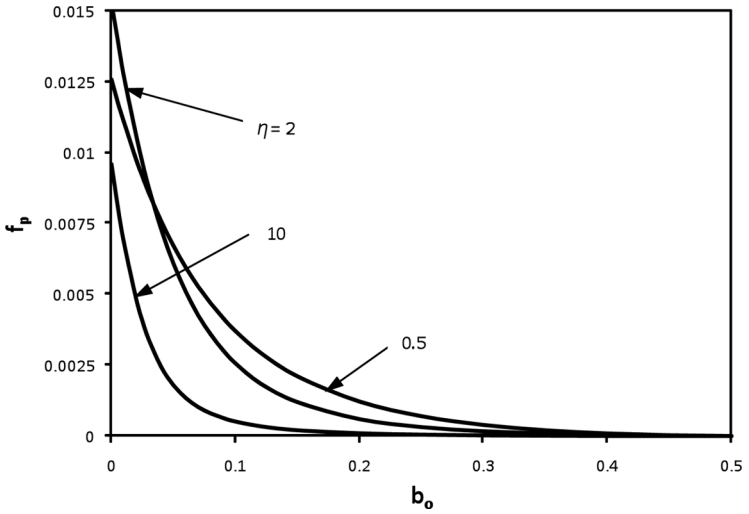

FIGURE 3 Peel force *versus* length of strip on left side without tape, for $\theta = 0.75\pi$, $s_o = 1$, $d_o = 0.5$, $g_c = 0.01$, and $\eta = 0.5$, 2, and 10.

$c_o = 0.7 - b_o$. When $b_o = 0$, $f_p = 0.0126$, 0.0175, and 0.0196, respectively, for $\eta = 0.5$, 2, and 10. For these three values, the peel force at $b_o = 0$ increases as the tape-to-strip stiffness ratio, η, increases, unlike the

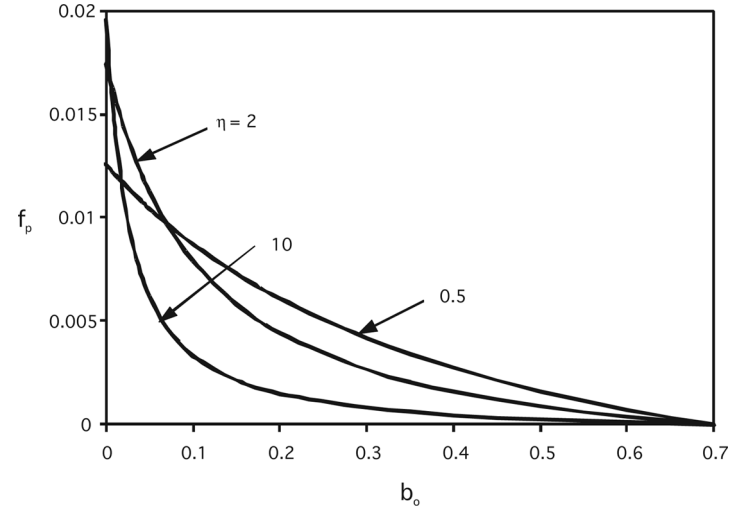

FIGURE 4 Peel force *versus* length of strip on left side without tape, for $\theta = 0.5\pi$, $s_o = 1.4$, $d_o = 0.7$, $g_c = 0.01$, and $\eta = 0.5$, 2, and 10.

situation in Fig. 3 where the peel force at $b_o = 0$ is lowest for $\eta = 10$. This type of behavior and the intersections of curves in Figs. 3 and 4 are due to the fact that f_p is not a monotonic function of η, which will be demonstrated in Section 3.3.

3.2. Effect of Initial Slack

Now the effect of initial slack is investigated. For the numerical results in this subsection, the peak of the initial configuration is at the center of the span (*i.e.*, $b_o + c_o = d_o = 0.5s_o$), and the attached length of the tape is fixed at $c_o = 0.4$ (so that $b_o = 0.5s_o - 0.4$). Results are presented in Fig. 5 for $g_c = 0.01$, $\eta = 10$, and $\theta = 0.5\pi$, 0.625π, and 0.75π, with the slackness parameter in the range $1 \le s_o \le 2$.

As s_o increases from unity (no initial slack), the peel force increases and then decreases. For $\theta = 0.5\pi$, 0.625π, and 0.75π, respectively, $f_p = 0.000471$, 0.000460, and 0.000513 when $s_o = 1$, and the maximum value of f_p is 0.00133 (at $s_o = 1.07$), 0.00114 (at $s_o = 1.05$), and 0.00103 (at $s_o = 1.03$). Therefore, except when the amount of slack is very small, f_p decreases as s_o increases in Fig. 5.

For the case $\theta = 0.75\pi$ in Fig. 5, the peel force decreases to zero when $s_o = \sqrt{2}$. At this point, the angles α and β in Fig. 1(b) are 0.25π and the force is collinear with the right side of the strip. The axial force in

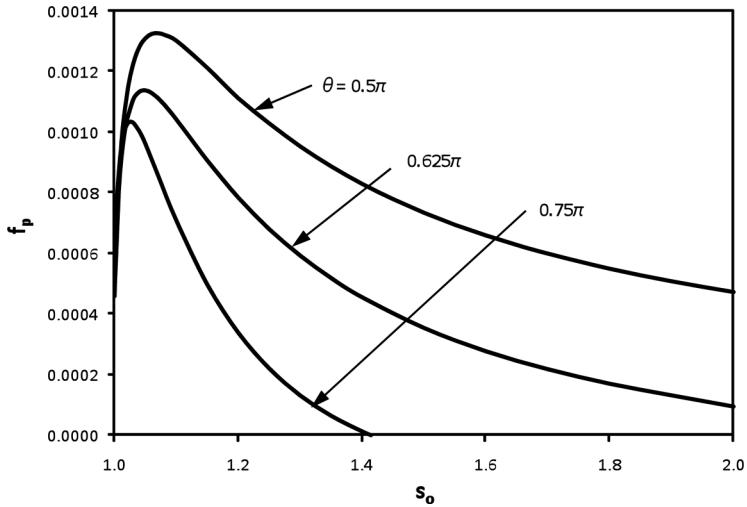

FIGURE 5 Peel force *versus* slackness parameter for $b_o = 0.5s_o - 0.4$, $c_o = 0.4$, $d_o = 0.5s_o$, $g_c = 0.01$, $\eta = 10$, and $\theta = 0.5\pi$, 0.625π, and 0.75π.

the left side of the strip is zero, and if s_o were increased beyond $\sqrt{2}$, this force would become negative, corresponding to compression, which is not permissible in the model under investigation. For $\theta = 0.625\pi$, the curve decreases to $f_p = 0$ when $s_o = 2.61$ (out of the range of the figure), and, in general, for any peel angle larger than 0.5π, the peel force decreases to zero at some value of initial slack.

In all subsequent examples, $b_o = 0$, *i.e.*, the tape is attached to the entire left side of the strip in Figs. 1(a) and (b). Equation (7) and the quantities b, Δb, b', ε_b, n_b, U_b, and ΔU_b are ignored in the analysis, and the coefficient k_α in Eqs. (11) and (12) is given by $k_\alpha = k_1/k_2$, where

$$k_1 = [2(1+\eta)d_o d - (d_o - 2d)c_o]\sin(\theta - \alpha) + c_o d_o \sin(\theta + \alpha + 2\beta), \quad (18)$$

$$k_2 = [2(1+\eta)(c_o - c)d_o d + (d_o - 2d)c_o c]\cos(\theta - \alpha) + c_o d_o c \cos(\theta + \alpha + 2\beta). \quad (19)$$

In Eqs. (18) and (19), note that $\theta - \alpha$ is the local peel angle ϕ, and $\theta + \alpha + 2\beta$ can be written as $\phi - 2\psi + 2\pi$ where $\psi = \pi - \alpha - \beta$ is the angle under the peak of the strip in Fig. 1(b), between the left and right sides.

3.3. Effect of Stiffness Ratio

In this subsection, the peel force is plotted as a function of the stiffness ratio, η, for the range $0.01 \le \eta \le 100$ (log scale). Three peel angles are considered: $\theta = 0.5\pi$, 0.625π, and 0.75π.

In Fig. 6, $s_o = 1$ (no initial slack), $c_o = d_o = 0.5$, and $g_c = 0.01$, whereas $s_o = 1.4$, $c_o = d_o = 0.7$, and $g_c = 0.01$ in Fig. 7. The values of the peel force for $b_o = 0$ are included in these figures, and it can be seen why f_p sometimes increases and sometimes decreases as η increases. The curves in these figures exhibit a maximum value of the peel force, and the corresponding value of η decreases as the peel angle increases in both of these figures. The maximum values of f_p for $\theta = 0.5\pi$, 0.625π, and 0.75π, respectively, are 0.0337, 0.0218, and 0.0153 in Fig. 6, and 0.0202, 0.0118, and 0.00529 in Fig. 7.

Based on Figs. 6 and 7, as the dimensional product $E_t A_t$ for the tape increases from a small value, the peel force initially increases and then decreases. The peel force is small for very small and very large values of $E_t A_t$.

The stiffness ratio, η, is proportional to the thickness of the tape. For a rigid substrate, Satas [8] presented experimental results on the effect of the backing thickness of a pressure-sensitive adhesive

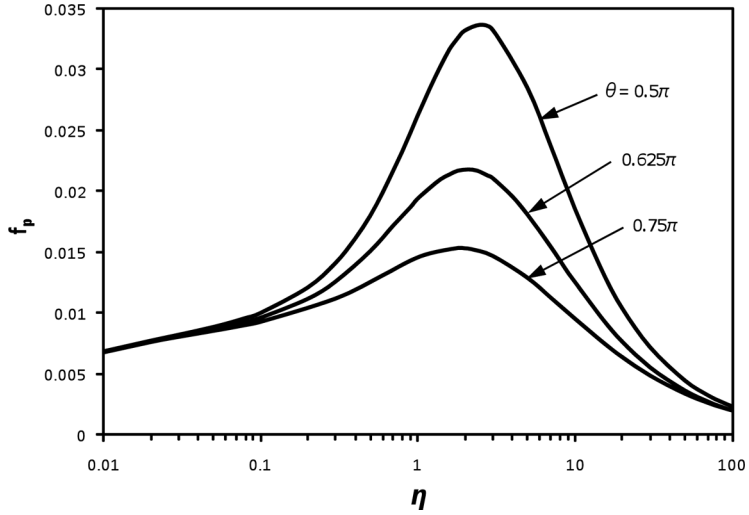

FIGURE 6 Peel force *versus* tape-to-strip stiffness ratio for $s_o = 1$, $c_o = d_o = 0.5$, $g_c = 0.01$, and $\theta = 0.5\pi$, 0.625π, and 0.75π.

tape on the peel force. As the backing thickness increased, in some cases the peel force increased, but in some others it increased and then decreased, as in Figs. 6 and 7.

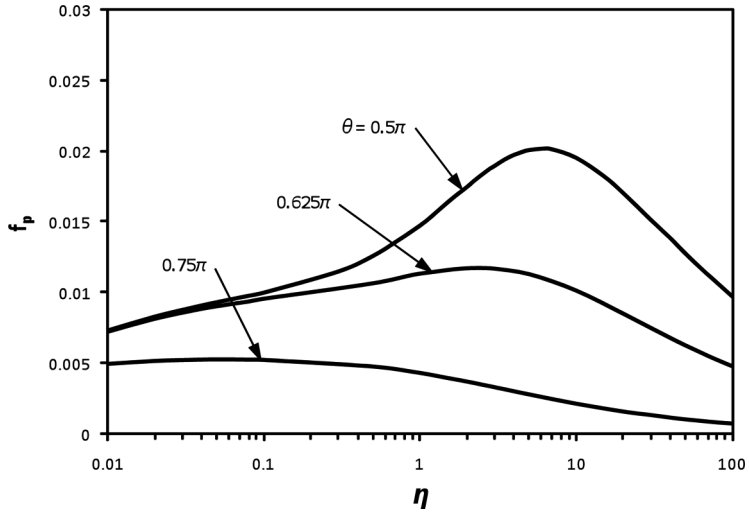

FIGURE 7 Peel force *versus* tape-to-strip stiffness ratio for $s_o = 1.4$, $c_o = d_o = 0.7$, $g_c = 0.01$, and $\theta = 0.5\pi$, 0.625π, and 0.75π.

3.4. Effect of Adhesive Fracture Energy

In this subsection, the effect of the nondimensional adhesive fracture energy, g_c, on the peel force, f_p, is investigated. Results are presented in Fig. 8 for $s_o = 1$, $c_o = d_o = 0.5$, $\eta = 10$, and $\theta = 0.5\pi$, 0.625π, and 0.75π. The range is $10^{-5} \le g_c \le 10^{-1}$ (log scale). As expected, f_p increases as g_c increases. For $\theta = 0.5\pi$, 0.625π, and 0.75π, respectively, the values of f_p are 0.0122, 0.00757, and 0.00498 for $g_c = 10^{-5}$, and 0.0537, 0.0365, and 0.0284 for $g_c = 10^{-1}$.

3.5. Effect of Peel Angle

The effect of θ, the angle of the force with the horizontal, is examined now. The peel force, f_p, is plotted *versus* θ/π in Figs. 9 and 10. In Fig. 9, $s_o = 1$ (no initial slack), $c_o = d_o = 0.5$, $\eta = 10$, and $g_c = 0.001$, 0.01, and 0.02. The range is $0.25\pi \le \theta \le 0.90\pi$. In Fig. 10, the strip is initially slack and the tape is again attached to half of the strip, with $s_o = 1.2$, $c_o = d_o = 0.6$, $\eta = 10$, $g_c = 0.001$, 0.01, and 0.02, and a range of $0.25\pi \le \theta \le 0.80\pi$.

Except for the initial portion of the bottom curve in Fig. 10, the peel force decreases as the peel angle increases in these results. For a rigid substrate, experimental results reported in [8–12] often exhibited a minimum peel force in the range $0.6 < \theta/\pi < 0.85$, but sometimes

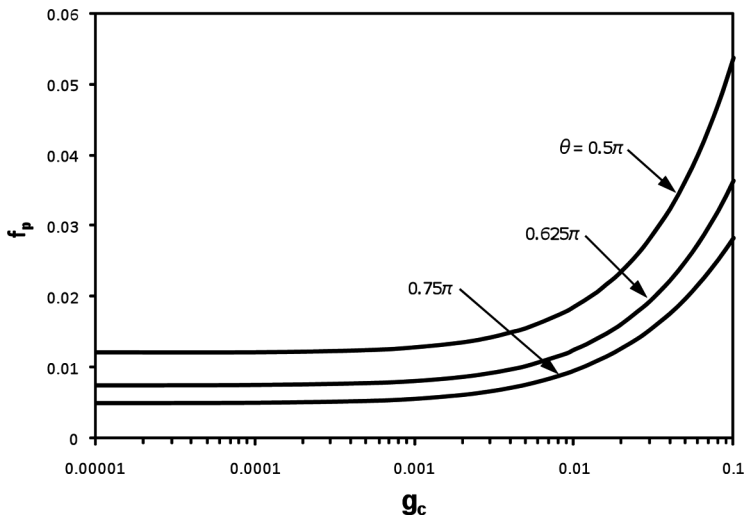

FIGURE 8 Peel force *versus* adhesive fracture energy for $s_o = 1$, $c_o = d_o = 0.5$, $\eta = 10$, and $\theta = 0.5\pi$, 0.625π, and 0.75π.

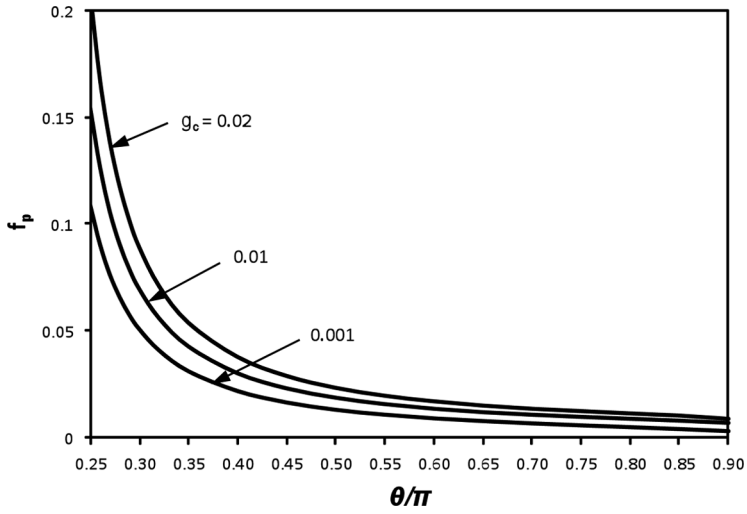

FIGURE 9 Peel force *versus* normalized peel angle for $s_o = 1$, $c_o = d_o = 0.5$, $\eta = 10$, and $g_c = 0.001$, 0.01, and 0.02.

showed a decreasing peel force. For peeling from human skin, test results were reported in [2] for $\theta/\pi = 0.5$, 0.67, 0.83, and 1. In most cases the lowest peel force occurred for $\theta/\pi = 0.83$, and in others it was observed for $\theta/\pi = 0.67$ or 1.

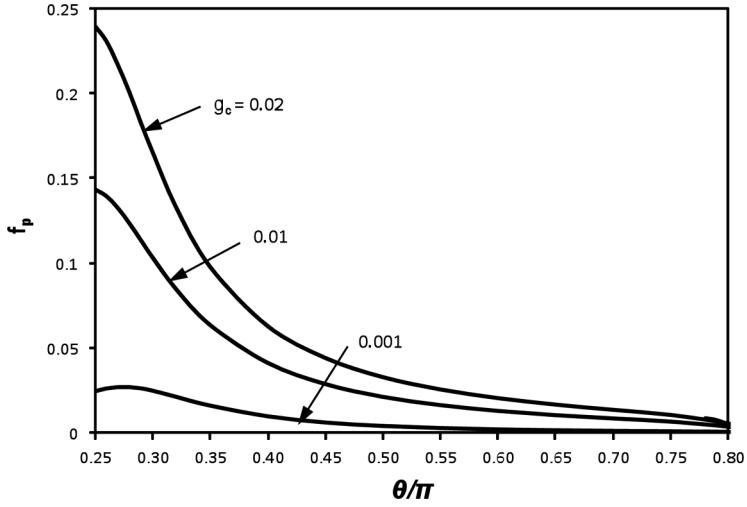

FIGURE 10 Peel force *versus* normalized peel angle for $s_o = 1.2$, $c_o = d_o = 0.6$, $\eta = 10$, and $g_c = 0.001$, 0.01, and 0.02.

4. INEXTENSIBLE TAPE

In some cases it may be appropriate to approximate the tape as having infinite axial stiffness (*i.e.*, being inextensible), as was done in Steven-Fountain *et al.* [5]. In Fig. 1, this means that $C = C_o$. The behavior of the strip before peeling occurs will be considered in this section for the case of an inextensible tape, as well as the conditions for peeling.

Equations (5) and (6) with $b = 0$ and $c = c_o$ lead to

$$d = \sqrt{(c_o \sin\alpha)^2 + (1 - c_o \cos\alpha)^2}. \tag{20}$$

With the use of Eqs. (4)–(6), (8), and (9), it can be shown that

$$f = \frac{\varepsilon_d \sin\alpha}{d \sin(\theta - \alpha)}. \tag{21}$$

Then, using Eqs. (3) and (20), Eq. (21) gives f as a function of α. [In [5], the equation that corresponds to Eq. (21) is incorrect.] Examples of the relationship in Eq. (21) are presented in Figs. 11 and 12 for $\theta = 0.75\pi$. The parameters are the same except that $s_o = 1$ in Fig. 11 and $s_o = 1.2$ in Fig. 12.

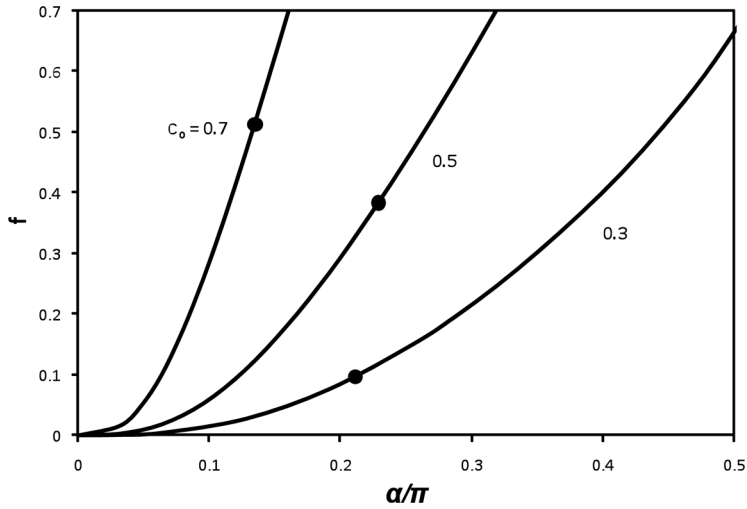

FIGURE 11 Applied force *versus* normalized left angle for inextensible tape, $\theta = 0.75\pi$, $s_o = 1$, $b_o = 0$, and $c_o = 0.3$, 0.5, and 0.7; dots indicate onset of peeling if $g_c = 0.01$.

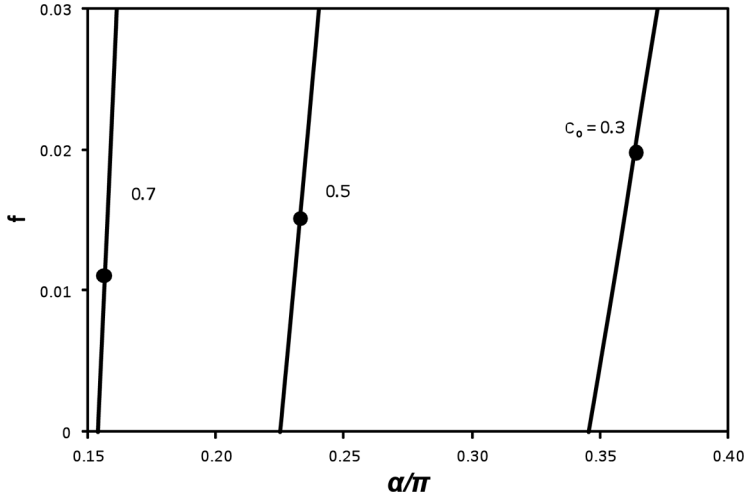

FIGURE 12 Applied force *versus* normalized left angle for inextensible tape, $\theta = 0.75\pi$, $s_o = 1.2$, $b_o = 0$, and $c_o = 0.3$, 0.5, and 0.7; dots indicate onset of peeling if $g_c = 0.01$.

When the strip is initially straight (Fig. 11), the curves start from the origin, since $\alpha_o = 0$. When there is initial slack, α_o can be computed from Eq. (20) with $d = d_o$. In Fig. 12, $\alpha_o = 0.345$, 0.225, and 0.154 for $c_o = 0.3$, 0.5, and 0.7, respectively.

To determine the peel force, f_p, Eq. (17) is included, with $\Delta U_b = \Delta U_c = \Delta U_r = 0$ and with the second term on the right side of Eq. (15) deleted in the formula for ΔW. Equation (17) can be evaluated to give the formula

$$g_c = f_p\left[1 - \cos(\theta - \alpha) + \tan\left(\frac{\alpha + \beta}{2}\right)\sin(\theta - \alpha)\right] - \frac{(d_o - d)(d_o - 3d)}{2d_o^2}. \tag{22}$$

In Eq. (22), $\theta - \alpha = \phi$, and $\tan[(\alpha + \beta)/2)]$ can be written as $\cot(\psi/2)$ where ψ is the angle under the peak in Fig. 1(b).

The dots in Figs. 11 and 12 indicate the peel force $f = f_p$ when $g_c = 0.01$. For this value of the nondimensional adhesive fracture energy, the segments of the curves above the dots would not be applicable. In Fig. 11, the dots are at $(\alpha_o/\pi, f) = (0.211, 0.0969)$ for $c_o = 0.3$, (0.229, 0.384) for $c_o = 0.5$, and (0.135, 0.514) for $c_o = 0.7$. In Fig. 12, they are at $(\alpha_o/\pi, f) = (0.364, 0.0198)$ for $c_o = 0.3$, (0.233, 0.0151) for $c_o = 0.5$, and (0.156, 0.0111) for $c_o = 0.7$.

If the substrate were rigid, the classical result [1] for an inextensible tape with negligible bending stiffness, in terms of the present nondimensional quantities, is $g_c = f_p\,(1-\cos\theta)$. This is obtained from Eq. (22) by setting $\alpha=\beta=0$ and $d=d_o$, and the resulting peel force decreases with peel angle in a manner similar to that in Fig. 9.

5. INEXTENSIBLE STRIP

5.1. Constant Peel Angle θ

In contrast to the previous section, here the strip (not the tape) is assumed to be inextensible (*i.e.*, in Fig. 1, $C=C_o$ and $D=D_o$, along with $B=B_o=0$; also, $\alpha=\alpha_o$ and $\beta=\beta_o$). Only the detached segment of the tape stretches as the force is applied. A similar analysis was conducted in Roop *et al.* [4].

In this section, the nondimensional quantities f^*, f_p^*, and g_c^* defined in Eqs. (1) are used, in which the axial stiffness of the tape is utilized instead of the axial stiffness of the strip (which is infinite). A similar modification is made for the nondimensional axial forces. Equations (5) and (6) are solved for the end angles, and Eqs. (8), (9), and (17) with $\Delta U_b=\Delta U_c=\Delta U_d=0$ lead to the following quadratic equation for the peel force f_p^*:

$$g_c^* = f_p^*\left[1-\cos(\theta-\alpha)+\tan\left(\frac{\alpha+\beta}{2}\right)\sin(\theta-\alpha)\right]+\frac{1}{2}(f_p^*)^2. \qquad (23)$$

As described after Eq. (22), Eq. (23) can also be written in terms of ϕ and ψ. When f_p^* is small (as in the following examples), the last term in Eq. (23) may become negligible, and then f_p^* becomes approximately proportional to the adhesive fracture energy.

Results for a constant peel angle, θ, are presented in Figs. 13 and 14, where $\theta=0.5\pi$, $g_c^*=0.001$, and three values of the slackness parameter are considered ($s_o=1.1$, 1.3, and 1.5). The normalized peel force, $10^3 f_p^*$, is plotted *versus* the attached length of the tape, c_o, in Fig. 13. If c_o is increased, the left angle, α_o, decreases and the local peel angle $\phi=0.5\pi-\alpha_o$ increases, which helps explain why the peel force decreases as c_o increases. If one envisions the progression of peeling as the tape is pulled, the attached length, c_o, decreases and the peel force increases.

Sometimes the peel force is plotted as a function of the displacement of the force. Here the total nondimensional length of the tape is assumed to be unity, and initially the entire tape is attached to the strip (corresponding to the right edge of Fig. 13). The height of the force above the supports is denoted δ, and at the beginning of peeling

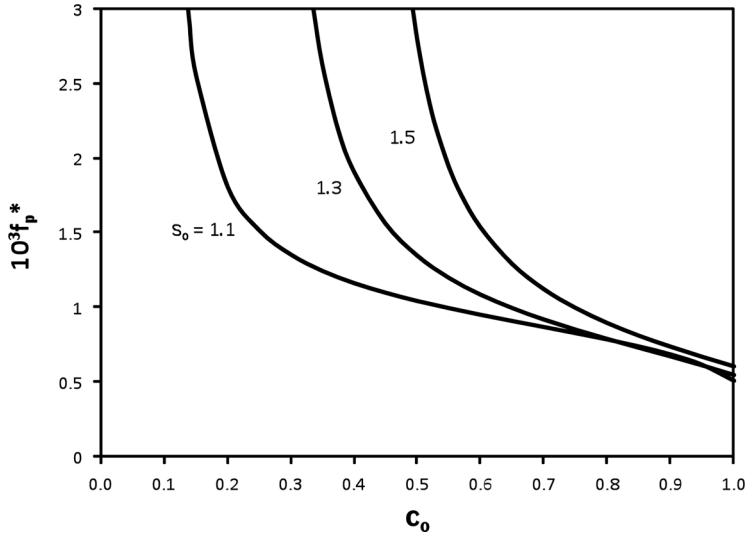

FIGURE 13 Peel force *versus* attached length of tape for inextensible strip, $\theta = 0.5\pi$, $b_o = 0$, $g_c^* = 0.001$, and $s_o = 1.1$, 1.3, and 1.5.

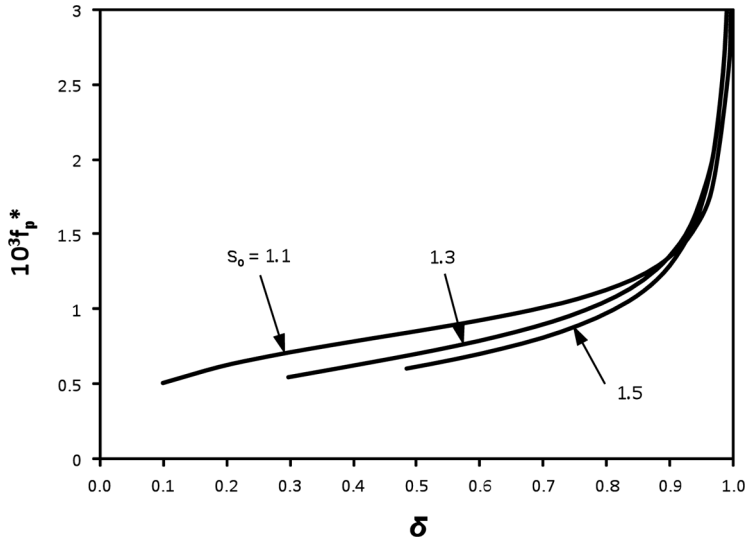

FIGURE 14 Peel force *versus* height of force above supports, as peeling progresses, for inextensible strip, $\theta = 0.5\pi$, $c_o = 1$ initially, $g_c^* = 0.001$, and $s_o = 1.1$, 1.3, and 1.5.

it is the height of the strip, which is $h_o = c_o \sin \alpha_o$, plus $1 - c_o$. As peeling progresses, the detached part of the tape stretches and δ is given by

$$\delta = c_o \sin \alpha + \left(1 + f_p^*\right)(1 - c_o). \tag{24}$$

In Fig. 14, $10^3 f_p^*$ is plotted as a function of δ. The curves for $s_o = 1.1$, 1.3, and 1.5, respectively, begin at $(\delta, 10^3 f_p^*) = (0.0999, 0.514)$, (0.297, 0.551), and (0.484, 0.608). The peel force becomes very large as the left angle, α, increases toward 0.5π, the value of θ. At $\delta = 1$, for $s_o = 1.1$, 1.3, and 1.5, respectively, $10^3 f_p^* = 4.09$, 5.17, and 5.75, $\alpha = 0.423\pi$, 0.451π, and 0.462π, and $c_o = 0.122$, 0.301, and 0.452.

If the substrate were rigid, the classical result [1] for a linearly elastic tape with negligible bending stiffness, in terms of the present nondimensional quantities, is obtained from Eq. (23) by setting $\alpha = \beta = 0$. The resulting peel force decreases with peel angle in a manner similar to that in Fig. 9.

5.2. Constant Local Peel Angle ϕ

In the previous examples, the peel angle, θ, between the force and the horizontal was fixed. In practice, with displacement control, the local peel angle, $\phi = \theta - \alpha$, between the force and the left side of the strip [Fig. 1(b)] may be kept constant (or approximately constant) as peeling progresses (*e.g.*, when peeling a medical adhesive off skin).

In the numerical results in this subsection, $g_c^* = 0.001$. For Fig. 15, peeling is initiated with a vertical force (i.e., $\theta = \theta_p = 0.5\pi$) and with $c_o = d_o = 0.5 s_o$. The initial peel force, f_p^*, is computed and the corresponding angle, $\alpha = \alpha_p$, is determined. The local peel angle for this initial peeling is $\phi_p = \theta_p - \alpha_p$. Then ϕ is fixed at this value and θ is written as $\phi + \alpha$. The left length, c_o, is specified (lower than $0.5 s_o$), d_o is given by $s_o - c_o$, α and β are computed from Eqs. (5) and (6), and f_p^* is obtained from Eq. (23). In Fig. 15, $10^3 f_p^*$ is plotted as a function of the normalized left angle α/π for $s_o = 1.1$, 1.2, and 1.3. As peeling progresses, α increases and the peel force decreases. The curves are ended when the force is horizontal (*i.e.*, $\theta = \pi$).

For the lowest curve, with $s_o = 1.1$, peeling begins when $\alpha_o = 0.137\pi$ and $10^3 f_p^* = 1.00$. Hence, $\phi = 0.363\pi$ for this case. At the end of the curve, $\alpha = 0.637\pi$, $10^3 f_p^* = 0.476$, and $c_o = 0.0692$. For the middle curve, with $s_o = 1.2$, $\phi = 0.314\pi$. At the top of the curve, $\alpha = 0.186\pi$ and $10^3 f_p^* = 1.00$, and at the bottom, $\alpha = 0.687\pi$, $10^3 f_p^* = 0.455$, and $c_o = 0.126$. For the top curve, $s_o = 1.3$ and $\phi = 0.279\pi$. The curve goes from $\alpha = 0.221\pi$ and $10^3 f_p^* = 1.00$ to $\alpha = 0.721\pi$ and $10^3 f_p^* = 0.435$ (with $c_o = 0.178$).

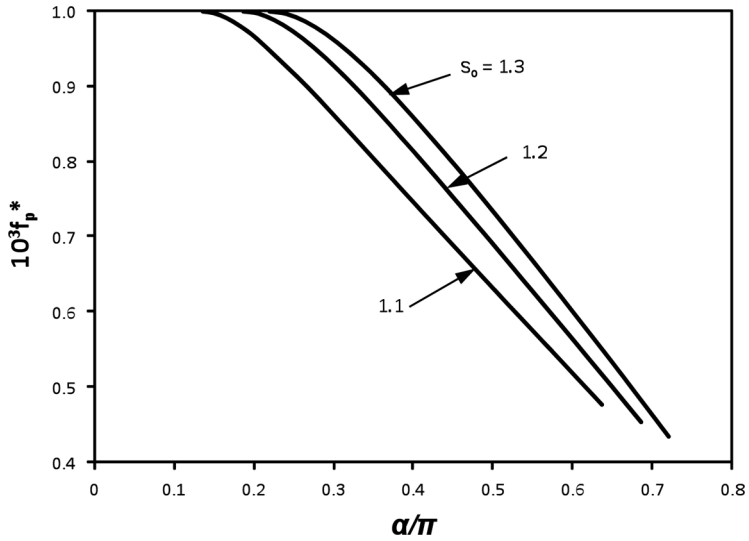

FIGURE 15 Peel force *versus* normalized left angle, with constant local peel angle ϕ, for inextensible strip, $g_c^* = 0.001$ and $s_o = 1.1$ ($\phi = 0.363\pi$), 1.2 ($\phi = 0.314\pi$), and 1.3 ($\phi = 0.279\pi$).

In Fig. 16, the tape is initially attached to 90% of the strip (*i.e.*, $c_o = 0.9s_o$, $d_o = 0.1s_o$) rather than half the tape. The slackness parameter is $s_o = 1.1$ and the initial left end angle is $\alpha_o = 0.035\pi$. Local peel angles of $\phi = 0.25\pi$, 0.5π, and 0.75π are considered, and the initial peel angle θ_o is $\phi + \alpha_o$. As peeling progresses, the peel force increases until the tape is attached to half the tape, and then decreases as the attached length decreases further. At the maxima in Fig. 16, $\alpha/\pi = 0.137$ and, for $\phi = 0.25\pi$, 0.5π, and 0.75π, respectively, $10^3 f_p^* = 1.62$, 0.686, and 0.492. At the left end of the three curves, $10^3 f_p^* = 1.025$, 0.509, and 0.418, respectively. At the right end, $\theta = \pi$, $\alpha = \pi - \phi$, $10^3 f_p^* = 0.476$, and, for $\phi = 0.25\pi$, 0.5π, and 0.75π, respectively, $c_o = 0.058$, 0.095, and 0.267.

If the peel force were plotted as a function of the length, c_o, of the left side of the strip, the curve would be symmetric about its maximum at $c_o = 0.5s_o$, even though the peel angle, θ, is different for two configurations that are mirror images across the center. Equation (23) depends on $\theta - \alpha$, which is the fixed value of ϕ, and on $\alpha + \beta$, which is the same for such a pair of shapes since α and β are interchanged. The strip is inextensible, so that the additional stiffness on the left side does not have an effect. Nevertheless, it seems to be surprising that the mirror-image shapes with different peel angles, θ (but the same local peel angle ϕ), have the same peel force. For the case in Fig. 16

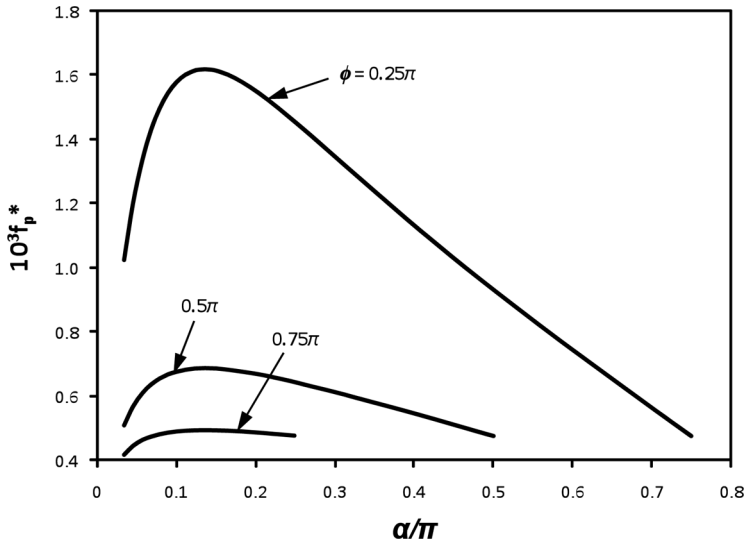

FIGURE 16 Peel force *versus* normalized left angle, with constant local peel angle ϕ, for inextensible strip, $s_o = 1.1$, $g_c^* = 0.001$, and $\phi = 0.25\pi$, 0.5π, and 0.75π.

with $\phi = 0.5\pi$, for example, if $c_o = 0.3$, then $d_o = 0.8$, $\alpha/\pi = 0.230$, $\beta/\pi = 0.080$, $h = 0.198$, $10^3 f_p^* = 0.654$, and $\theta/\pi = 0.730$, and for the mirror-image shape, $c_o = 0.8$, $d_o = 0.3$, $\alpha/\pi = 0.080$, $\beta/\pi = 0.230$, $h = 0.198$, $10^3 f_p^* = 0.654$, and $\theta/\pi = 0.580$ (*i.e.*, c_o and d_o are interchanged, α and β are interchanged, ϕ is fixed, and then f_p^* remains the same even though θ changes).

For the curves in Fig. 15 and the top curve in Fig. 16, the left angle, α, of the strip becomes significantly larger than 0.5π. In Fig. 1(b), the peak of the strip would then be to the left of the left support.

If the strip were extensible, the type of analysis in this subsection for the case of constant local peel angle would not be applicable. The work done by the force would be dependent on its path, the system would be nonconservative, and Eqs. (15) and (17) would not be valid. For an inextensible strip, however, the configuration is known if, for example, α is given, and the work done by the force when the system moves from one configuration to another is fixed.

6. EXPERIMENTAL RESULTS

Experiments were conducted in which the tape was Johnson & Johnson (New Brunswick, NJ, USA) Waterproof First Aid tape with thickness 0.25 mm, width 12.7 mm, and Young's modulus 0.6 GPa, so

that $E_tA_t = 1.9\,\text{kN}$. The strip was transparency film with thickness 0.07 mm, width 25.4 mm, and Young's modulus 4 GPa. Using the effective film width to be the width of the tape, $E_sA_s = 3.5\,\text{kN}$. Hence, the tape-to-strip stiffness ratio was $\eta = 0.54$.

The span of the standard machinist vise was $L = 6.3\,\text{cm}$, and the vise was placed on the platform of an Instron 4505 tensile testing machine. The peel angle was maintained at $\theta = 0.5\pi$ by moving the vise horizontally as the platform moved downward and the tape peeled from the film. Data on peel force and platform displacement were collected using LabView^{TM} software.

Results for the slackness parameter $s_o = 1.11$ were presented in [4]. Tests were run with three different downward velocities of the platform: 30, 90, and 150 mm/min. The peel force during the initial part of the peeling process was approximately 1.0, 1.3, and 1.6 N, respectively, for these three peel rates, and the behavior resembled that in Fig. 14.

Results for $s_o = 1.25$ are shown in Fig. 17 for the same three peel rates. The peel force is plotted as a function of its upward displacement, and is higher for a higher peel rate. As in most of the runs, an early peak occurs when peeling begins, and thereafter the peel force tends to increase as peeling progresses. If the analysis in Section 2 is carried out for $s_o = 1.25$, $b_o = 0$, $c_o = 0.5$, $\eta = 0.54$, and $g_c = 10^{-4}$ (corresponding to $G_c = 28\,\text{J/m}^2$), one obtains $f_p = 0.00015$, $F_p = 0.51\,\text{N}$, and a force displacement (*i.e.*, extension) of 50 mm, which is comparable with the result in Fig. 17 for the lowest peel rate.

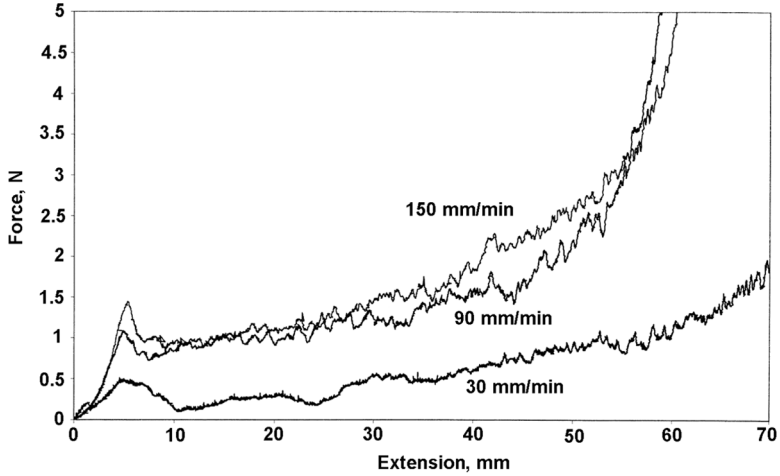

FIGURE 17 Experimental peel force *versus* upward displacement of force, as peeling progresses, for peel rates 30, 90, and 150 mm/min.

Some tests were also conducted with a peel angle $\theta = \pi$, and the resulting peel force was lower than for the case of vertical loading ($\theta = 0.5\pi$).

7. CONCLUDING REMARKS

Peeling of a pressure-sensitive tape from a thin strip with fixed ends was analyzed. The strip was either straight or slack prior to a force being applied to the detached end of the tape. It was assumed that the strip and tape were linearly elastic and had negligible bending stiffness, self-weight, and prestress. Three-dimensional effects were neglected, and quasi-static steady peeling was assumed (so that the peel rate was not involved). The tape was pulled with either a constant angle with respect to the horizontal line between the supports (*i.e.*, constant peel angle) or a constant angle with respect to the side of the strip to which the tape was attached (*i.e.*, constant local peel angle).

The peel force was determined based on the standard criterion from fracture mechanics that involves the adhesive fracture energy (*i.e.*, the critical value of the strain energy release rate), G_c. It was assumed that G_c was independent of the peel angle, configurations of the strip and tape, and axial stiffnesses of the strip and tape.

The nondimensional peel force, f_p (or f_p^*), depends on various parameters, such as the ratio, η, of the axial stiffnesses between the tape and the strip, the nondimensional adhesive fracture energy, g_c (or g_c^*), the ratio, s_o, of the initial strip length to the span (*i.e.*, the slackness parameter), the peel angle, θ, the local peel angle, ϕ, and the initial placement of the tape on the strip (defined by b_o, c_o, and d_o).

Based on this analysis, some conclusions can be drawn. The peel force increases as the adhesive fracture energy increases. As the slack of the strip increases, the peel force tends to initially increase and then to decrease. This type of behavior also tends to occur as the tape-to-strip stiffness ratio is increased. A maximum also occurs for an inextensible strip as peeling progresses if the initial tape is longer than half the strip length and the local peel angle, ϕ, is kept constant. For initial peeling, the analysis predicts that the peel force is usually smaller if the peel angle, θ, is larger.

If all conditions are the same except for the attached length, c_o, of the tape, the peel force tends to increase as c_o increases. However, if the tape is peeled off the strip with constant peel angle, the attached length decreases but the configuration changes, and the peel force tends to increase.

An experimental result was presented in which the peel force increased as peeling progressed, and was higher if the peel rate was higher.

The analysis could be extended to model the case of nonlinear stress-strain relationships for the strip and the tape. Equations (4), coefficients k_b, k_d, k_α, and k_β in Eqs. (11) and (12), and Eqs. (13)–(15) for the energies and work would be modified. In [5], the strip under investigation was made of latex rubber, which is a softening material (*i.e.*, its axial stiffness decreases as the applied tension is increased). If the strip were to represent skin, its stress-strain relationship would be hardening. One can consider the model utilized in the present study when the strip is initially slack (*i.e.*, $s_o > 1$) to represent a simple bilinear constitutive law for a hardening material, with zero stiffness for an initial phase of stretching and then constant stiffness for subsequent stretching.

Other extensions of this analysis would also be useful. Forces that resist upward deformation between the ends of the strip could be included, along with bending stiffness, self-weight, and prestress of the strip and tape. A finite element analysis could be performed to include three-dimensional effects, such as the curvature of the peel front (with the highest attached point of the strip typically being at the center of the tape and the lowest being at the edges). Time-dependent effects could be included, in particular, the viscoelastic characteristics of pressure-sensitive adhesives. Plastic behavior of the tape is important in some cases of peeling. Alternative peeling criteria could be considered. Further experimental results could determine the applicability of the considered two-dimensional model. The present study has extended the work of [4,5] to include both extensible strips and tapes, a large range of peel angles, and strips that are initially slack, but much more research is needed on peeling of adhesive tapes from thin, flexible substrates.

ACKNOWLEDGMENT

The author is grateful to the reviewers for their helpful comments.

The author is grateful to Dr. David A. Dillard for his collaboration and leadership on research problems in the field of adhesion.

REFERENCES

[1] Kinloch, A. J. and Williams, J. G., The mechanics of peel tests in *The Mechanics of Adhesion*, D. A. Dillard and A. V. Pocius (Eds.) (Elsevier, Amsterdam, 2002), pp. 273–301.

[2] Karwoski, A. C. and Plaut, R. H., *Skin Research Technol.* **10**, 271–277 (2004).

[3] Plaut, R. H. and Karwoski, A. C., *Proceedings of the 18th ASCE Engineering Mechanics Division Conference*, M. R. Hajj (Ed.) (Blacksburg, Virginia, 2007).

[4] Roop, R. V., Plaut, R. H., Dillard, D. A., and Ohanehi, D. C., *Proceedings of the 25th Annual Meeting of the Adhesion Society and the Second World Congress on Adhesion and Related Phenomena (WCARP-II)*, (Orlando, Florida, 2002), pp. 129–131.
[5] Steven-Fountain, A. J., Atkins, A. G., Jeronimidis, G., Vincent, J. F. V., Farrar, D. F., and Chivers, R. A., *Int. J. Adhesion Adhesives* **22**, 423–430 (2002).
[6] Wolfram, S., *Mathematica: A System for Doing Mathematics by Computer*, (Addison-Wesley, Reading, Massachusetts, 1991).
[7] Maugis, D., *Contact, Adhesion and Rupture of Elastic Solids*, (Springer-Verlag, Berlin, 2000).
[8] Satas, D., Peel in *Handbook of Pressure Sensitive Adhesive Technology*, D. Satas (Ed.) (Satas and Associates, Warwick, Rhode Island, 1999), 3rd ed., pp. 62–86.
[9] Aubrey, D. W., Welding, G. N., and Wong, T., *J. Applied Polymer Sci.* **13**, 2193–2207 (1969).
[10] Dahlquist, C. A., Pressure-sensitive adhesives in *Treatise on Adhesion and Adhesives*, R. L. Patrick (Ed.) (Marcel Dekker, New York, 1969), Vol. 2, pp. 219–260.
[11] Kaelble, D. H., in *Handbook of Pressure Sensitive Adhesive Technology*, D. Satas (Ed.) (Satas and Associates, Warwick, Rhode Island, 1999), 3rd ed., pp. 87–120.
[12] Chivers, R. A., *Int. J. Adhesion Adhesives* **21**, 381–388 (2001).